CLIMA 2016 - proceedings of the 12th REHVA World Congress

volume 3

Heiselberg, Per Kvols

Publication date:
2016

Document Version
Publisher's PDF, also known as Version of record

Experimental Analysis of a Gas Micro-Cogeneration Based on Internal Combustion Engine and Calibration of a Dynamic Model for Building Energy Simulation

Romain Bonabe de Rougé[#°1], Thomas Tirtiaux[*], Pierre Picard[°*2], Pascal Stabat[#], Dominique Marchio[#]

[#]*Centre for Energy efficiency of Systems, Mines ParisTech*
60 Bd Saint-Michel, F-75272 Paris CEDEX-06, FRANCE

[°]*Efficacity*
14-20 boulevard Newton, Champs-sur-Marne, 77447 Marne la Vallée CEDEX, FRANCE

[1]r.bonabederouge@efficacity.com

[*]*CRIGEN, Engie*
361, Avenue du Président Wilson - BP. 33, 93211 La Plaine Saint-Denis, FRANCE

[2]pierre-2.picard@engie.com

Abstract

Internal combustion engine (ICE)-based micro-cogeneration (µCHP) covers a wide range of capacities and recent developments increased the efficiency through condensing exhaust device and variable speed pumps. This type of equipment is suitable for residential and commercial buildings and is usually integrated in a system with back-up boiler. A dynamic model is required to investigate the seasonal energy performance of these equipments. A generic grey-box model with few and easily accessible parameters has been developed to simulate the dynamics of the heat and electricity productions of an ICE-based µCHP. The unit under scope develops an electrical power of 7.5 kW and a thermal power of 20 kW. The test facility is described and the uncertainty of the measurement chain is assessed. The static and dynamic parameters of the micro-cogeneration model have been identified based on a set of experimental data representative of all operating conditions. The model will be used to undertake building energy simulation studies in various cases such as collective housing, commercial buildings, hotels to identify the optimal sizing of components (µCHP, back-up, storage) and controls for various tariffs (self-consumption, feed-in, sale-back) .

Keywords – micro-cogeneration ; internal combustion engine ; model calibration ; experimentation

1. Introduction

Context

Many actions are actually set to reduce the energy demand of buildings such as improving wall insulation and air tightness, producing electricity and heat for buildings more efficiently. Micro-Combined Heat and Power (µCHP) is an innovative technology for distributed electricity production (power rating below 50 kWel). From one side, the

heat production is recovered thanks to the space heating and/or domestic hot water production system of a building. From the other side, the produced electricity can be self-consumed if there is a concomitant electrical need or exported to the electrical network. It results that µCHPs can produce electricity with high primary energy efficiency [1]. However, the thermal energy needs to be totally consumed in the building. It is critical to produce as much electricity as possible for a given thermal need, to reduce the primary energy demand and the energy bill of the building.

The dynamics of thermal and electricity needs in residential and small commercial buildings are often studied in literature and both show strong time-variability that are not always simultaneous. That is why sizing and controlling µCHP systems is not trivial and need to be investigated. Moreover, an auxiliary burner is generally added for peak heat demands (electricity grid plays a similar role for the electrical demand). The designer issues are the proper sizing of each equipment, their control, the need for thermal and/or electrical storage, the economic impact of electricity tariffs (feed-in vs self-consumption), the potential of flexibility in a smart grid, etc.

Methods

For this type of applications, literature shows [3] [4] that dynamic models of µCHP used in building energy simulation programs such as TRNSYS, Dymola [2], EnergyPlus are suitable. That is why a generic grey-box model has been developed with few and easily accessible parameters. It has already been used to represent Stirling Engines with success [5] and slightly modified for a wood pellet Steam Engine [6]. This paper deals with parameterization of the same model for an Internal Combustion Engine (ICE) thanks to experimental investigations undertaken on a 7.5 kWel and 20 kWth unit. ICE-based µCHP are systems relying on a well-known technology which is similar to car motors supplemented by heat exchangers on exhaust gas, cooling loop and oil circuit.

To investigate the performance of the studied µCHP and calibrate the model, a review of literature and presentation of the model will be followed by a description of the test bench. Finally a discussion and a conclusion end the paper.

2. Modeling µCHP

State of the art

Three types of models can be distinguished for µCHP which do not aim the same types of applications.

Full physical models: this type of model relies on a detailed description of µCHP, including the combustion reaction, thermodynamic cycle, heat transfer models between the different parts of the machine and description of the process for electricity production. As discussed by [5], timesteps for this type of models are much lower to the ones used for building energy simulation, as a consequence they are not considered for our purpose.

Semi-physical models: these models are intended to represent operation of a µCHP keeping in mind that it is governed by physical laws but simplifying and/or grouping multiple phenomena with equations mixing physics and empirical parameters. Advantages are a better computational time and no need to describe every phenomena but it requires experimental investigation on machines to identify the calibration parameters. They are largely adopted [7] for these reasons and used in this paper.

Simplified model: this type of model, simplified and only taking into account a very few phenomena, is aimed at being used in optimal control problems for example (MPC, Dynamic Programing …). Advantages are a very fast computation time and only minimal information is required (basically manufacturers' data).

Semi-physical model description

The generic model is separated in two parts: transient behavior (start/stop phases) and steady-state operation.

The steady-state operation describes the gas consumption (P_{fuel}), heat production ($\dot{Q}_{HX}$) and electricity (P_{gross}) as a function of cooling water flow rate ($\dot{m}_{cw}$) and inlet water temperature ($T_{cw,i}$). Load level (C_{load}) has been added to the model [8] to represent ICE modulating behavior (1-3):

$$P_{fuel} = P_{fuel}^{nom} + a\left(T_{cw,i} - T_{cw,i}^{nom}\right) + b\left(\dot{m}_{cw} - \dot{m}_{cw}^{nom}\right) + k \cdot (1 - C_{load}) \quad (1)$$

$$\dot{Q}_{HX} = \dot{Q}_{HX}^{nom} + c\left(T_{cw,i} - T_{cw,i}^{nom}\right) + d\left(\dot{m}_{cw} - \dot{m}_{cw}^{nom}\right) + g \cdot (1 - C_{load}) \quad (2)$$

$$P_{gross} = P_{gross}^{nom} + e\left(T_{cw,i} - T_{cw,i}^{nom}\right) + f\left(\dot{m}_{cw} - \dot{m}_{cw}^{nom}\right) + h \cdot (1 - C_{load}) \quad (3)$$

Parameters "a" to "k" are used for calibration and nominal values of $\dot{m}_{cw}$ and temperature $T_{cw,i}$ are chosen according to manufacturers' data for example. Calibration should be carried out by observation of the three power variables when varying separately C_{load}, $T_{cw,i}$ and $\dot{m}_{cw}$ in all the operation range. In practice, for the studied machine, the influence of $\dot{m}_{cw}$ can be neglected because the pump-control of the µCHP maintains outlet temperature at a quasi-constant temperature of 85-90 °C by varying the flow rate to ensure optimal operating conditions. It means that for a given load level and a given return temperature, the flow rate is fixed unless the pump is unable to reach the desired flow rate (this case is unlikely to happen as the machine is normally connected to a tank). This particular behavior was modeled in the pump controller in order to correctly predict thermal exchange conditions (temperature and flow rate).

C_{load} is added to account for power modulation. The tested Internal Combustion Engine is able to go down to 50 % (3750 W) of its nominal electrical power. C_{load} is calculated with equation (4):

$$C_{load} = \frac{P_{gross}}{P_{gross}^{nom}} \quad (4)$$

Exhaust gas heat losses are separated in two terms, sensible and latent losses. Sensible losses depend on the exhaust temperature which is measured on the bench and fitted with a linear relation (5) depending on the cooling water inlet temperature. It was

observed that the load level had no relevant effect on the exhaust temperature (see Fig. 6).

Latent heat losses can be calculated thanks to the condensed water measured with a weighing machine. The model assumes a bounded linear relation between the condensate mass flow rate and the cooling water temperature and the fuel input (6). The remaining steady-state parameters are detailed in [5].

$$T_{exh} = k_{exh}\left(T_{cw,i} - T_{cw,i}^{nom}\right) + T_{exh}^{nom} \quad (5)$$

$$\dot{m}_{condens} = (k_{condens} \cdot T_{cw,i} + l_{condens}) \cdot \frac{P_{fuel}}{P_{fuel}^{nom}} \quad (6)$$

The transient operation equations describe start/stop phases and variation of internal temperature. To compute this temperature, a first order model is adopted writing the energy balance (7) of the machine as:

$$[MC]_{int} \cdot \frac{dT_{int}}{dt} = \dot{H}_{fuel} + \dot{H}_{air} + P_{fuel} - P_{gross} - \dot{Q}_{HX} - \dot{Q}_{loss} - \dot{H}_{exh}^{sens} - \dot{H}_{exh}^{lat} \quad (7)$$

While P_{gross}, P_{fuel} and $\dot{Q}_{HX}$ are computed thanks to equations (1-3), the enthalpy flux $\dot{H}_{fuel}$ and $\dot{H}_{air}$ are obtained thanks to the gas composition and assuming that a quasi-stoichiometric combustion takes place in the engine. This assumption is validated through measurements with a Lambda probe on the exhaust gas (air/fuel ratio of 1.01±0.1 times the stoichiometric conditions).

Thermal losses $\dot{Q}_{loss}$ are considered as proportional to the difference between the mean temperature of the water and the environment (8). The chosen form, including C_{load}, gives the best results when minimizing error between measurements and model while keeping some physical meaning in the equation. $[UA]_{loss}$ and k_{loss} coefficients in normal operation are obtained in the calibration process as $\dot{Q}_{loss}$ is the remainder of the energy balance in equation (7) in steady-state conditions.

$$\dot{Q}_{loss} = C_{load}\left([UA]_{loss}\left(\frac{T_{cw,o} - T_{cw,i}}{2} - T_{amb}\right) + k_{loss}\right) \quad (8)$$

$[UA]_{loss}$ and k_{loss} coefficients may be different during stand-by versus normal operation because thermal exchange conditions are changed. They are evaluated by calculating how much energy is needed to maintain motor temperature constant at various setpoints by circulating water in stand-by mode.

To obtain $[MC]_{int}$, two approaches were compared. The first is proposed by [8], τ_{RF} is evaluated observing the evolution of T_{int} during a cooling phase without circulation of cooling water. This evolution is assimilated to an exponential decay (9):

$$[MC]_{int} = [UA]_{loss} \cdot \tau_{RF} \quad (9)$$

The other possibility, which is proposed here is to assess a different $[UA]_{loss}$ during a cooling phase with water circulation. Knowing the evolution of $T_{cw,o}$, $T_{cw,i}$ and

T_{int} during a constant flow rate cooling phase (of about 3 minutes during the test), an mean "active" $[UA]_{loss}$ is determined (10). τ_{RF} is different during the active cooling phase and thus $[MC]_{int}$ is evaluated again. The two methods are remarkably close with a relative difference of 4.7 %.

$$[UA]_{loss}^{\text{active}} = \frac{\dot{Q}_{HX}}{T_{int} - \frac{T_{cw,o} - T_{cw,i}}{2}} \tag{10}$$

To describe start-up phases, an exponential form is adopted for $\dot{Q}_{HX}$ in equation (11) where t_{start} is the starting time and Δt_{start}^{Q} the delay before heat production.

$$\dot{Q}_{HX} = \begin{cases} 0 & if\ t < t_{start} + \Delta t_{start}^{Q} \\ \dot{Q}_{HX}^{nom} \left(1 - e^{-\frac{t - \left(t_{start} + \Delta t_{start}^{Q}\right)}{\tau_{start}^{Q}}} \right) & if\ t \geq\ t_{start} + \Delta t_{start}^{Q} \end{cases} \tag{11}$$

Required electrical power is instantaneously reached after a 10 second time-delay and no exponential equation is necessary.

During cooling phases, between normal operation and stand-by, some electrical energy is released for a few seconds after the stop. In the model, this amount of energy is spread during all the cooling phase. Even if the machine can enter in cooling phase after different values of $\dot{Q}_{HX}$, meaning that the heat released to the fluid during cooling could be different, an exponential form not depending on the previous state of operation is used (12).

$$\dot{Q}_{HX} = \begin{cases} 0 & if\ t > t_{stop} + \Delta t_{stop}^{Q} \\ \dot{Q}_{HX}^{nom} \cdot e^{-\frac{t - t_{stop}}{\tau_{stop}^{Q}}} & if\ t \leq\ t_{stop} + \Delta t_{stop}^{Q} \end{cases} \tag{12}$$

This assumption is validated thanks to measurements shown in Fig. 1 for stops after stationary loads of 13 to 18 kW. No significant correlation could be extracted from various cooling phases and previous operation conditions. This can be explained by the fact that between t_{stop} and $t_{stop} + \Delta t_{stop}^{Q}$, the pump is suddenly set to maximal speed. A part of the heat contained in the thermal mass of the engine is released to the water. In part load conditions, the pump works at low speed so the acceleration will strongly discharge the mass which is not the case at full load. This results in similar heat release in each case.

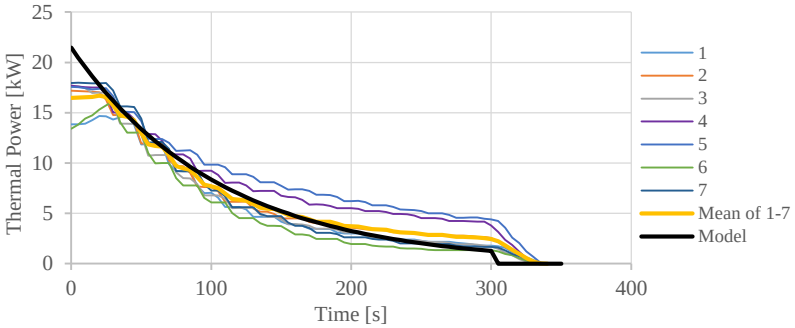

Fig. 1 Thermal power measured during 7 cooling phases of the µCHP, comparison to the mean of these series and the model

3. Experimental test bench description

The test bench (Fig. 2) was mounted in COSTIC facility in France.

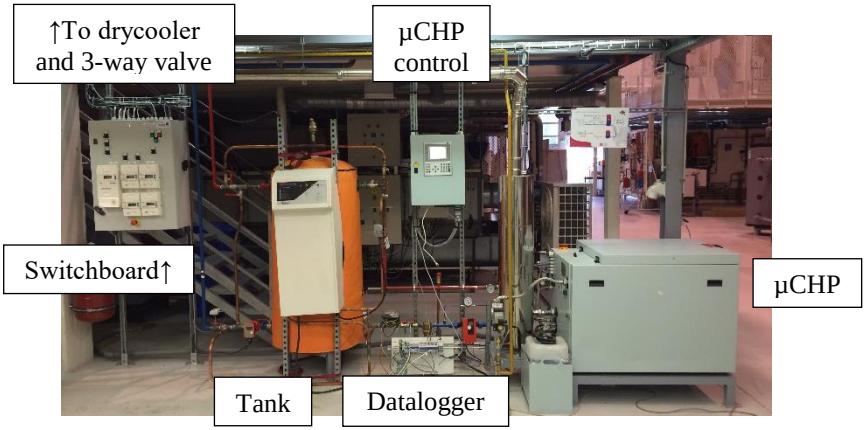

Fig. 2 Test facility (drycooler and 3-way valve are outside of the scope of the picture)

It is composed of a hot water storage and a drycooler with multiple hydraulic paths. The µCHP unit can store heat in the tank or it can directly throw heat production to the drycooler bypassing the tank. The tank can also be cooled by the drycooler while being charged. A PID controller is mounted with a 3-way valve to control return water temperature of the engine in order to observe steady-state operation in multiple fixed conditions. The main instruments and uncertainties values are given in Table 1. Relative uncertainties are given for a steady-state operation of 15 minutes.

Table 1. List of measuring equipement

	Type	Notation	Metrological means	Uncertainty
Fuel	Consumed Fuel	$\dot{V}_{fuel}$	Pulse counter	±1.7 % (calibrated) and 0.0002 m^3
	GHV	GHV	Gas supplier	±50 $Wh.m^{-3}$
	Fuel temperature	T_{fuel}	PT100	±2 K (estimated)
	Fuel power	P_{fuel}	Calculated	±2.9 %
Heating output	Inlet water temperature	$T_{cw,i}$	Paired PT100	±2.9 % on ΔT (calibrated)
	Outlet water temperature	$T_{cw,o}$		
	Vol. flow rate	$\dot{m}_{cw}$		±0.3 % (calibrated)
	Heat Power	$\dot{Q}_{HX}$	Calculated	3.3 % (calibrated)
Electrical output power		P_{gross}	Watt-meter	±1.0 % and 10 Wh
Exhaust gas temperature		T_{exh}	Gas analyzer	±0.5 K (calibrated)
Engine temperature		T_{int}	Engine sensor	±1 K
Ambient temperature		T_{amb}	PT100	±0.2 K (calibrated)

4. Experimental results and calibration

Steady-state operation

All the steady-state parameters are obtained for measurement conditions such as temperature is not varying of more than 1 K and power is not varying of more than 5 % around the target value. Fig. 3 shows that there is a good agreement between measures and model (dashed lines). Seven different load levels were tested and this was made for $T_{cw,i} = 40$, 50 and 60 °C. $T_{cw,i} = 30$ °C was also tested but the drycooler was not able to dissipate more than 10 kW at such a low temperature.

Fig. 4 shows the evolution of overall efficiency for multiple inlet water temperatures and load levels. Overall efficiency increases with diminution of load level and temperature. Indeed, the rise of efficiency for low water temperature and load level hides decreased electrical efficiency and increased thermal efficiency.

Fig. 5 shows the distribution of the production and losses in the unit for different load levels. It can be noted that for $T_{cw,i} =$ 60 °C, latent heat losses are quite important.

Finally, the evolution of exhaust gas temperature is shown on Fig. 6, variation of exhaust temperature against load level is not relevant (+0-3 K) in comparison with variation against inlet water temperature (+21 K) as it was decided for equation (5). Temperatures shown on the right indicate the setpoint for inlet water and may not be totally exact (±1 °C) depending on the quality of 3-way valve control.

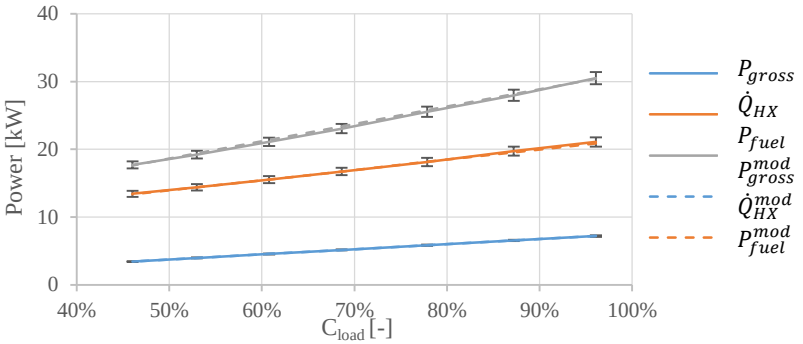

Fig. 3 Fuel consumption, electrical and thermal production for different load levels for 50 °C inlet water temperature

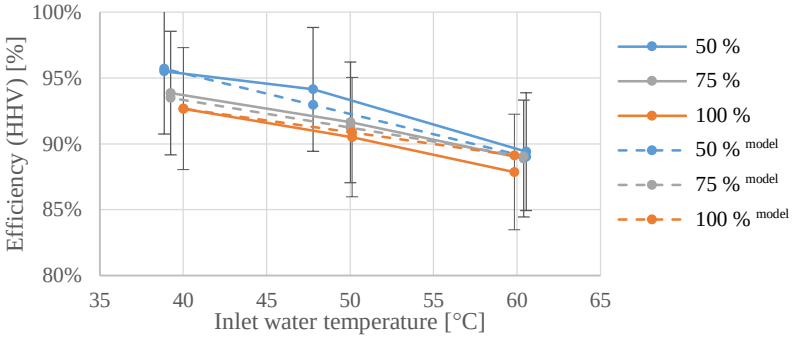

Fig. 4 Overall efficiency for 3 inlet water temperatures and 3 load levels (right caption)

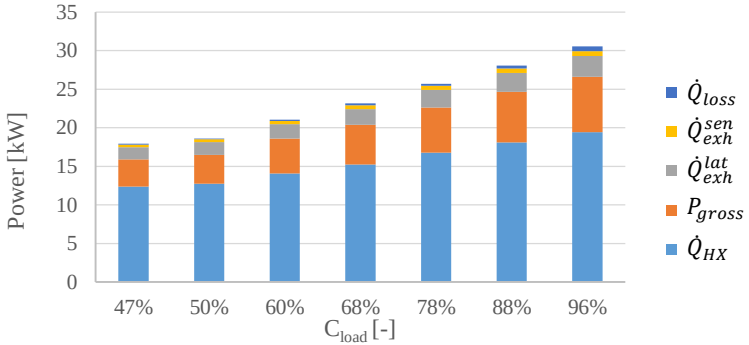

Fig. 5 Energy balance of the µCHP unit for different load levels and $T_{cw,i}$ = 60 °C, the total of each bar is gas consumption minus enthalpy of inlet air and gas (negligible)

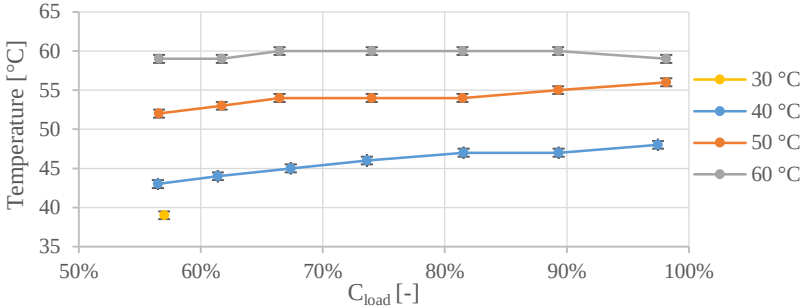

Fig. 6 Exhaust gas temperature versus inlet water temperature and load level

Start-up phase

Measurement were made on the evolution of thermal power during a start-up phase and were used to calibrate parameters of equation (11) minimizing cumulated square error, the result can be seen on Fig. 7. The relative error in energy is lower than 1 %. Concerning gas consumption, a constant value is applied during start-up as no over-consumption during start-up was observed. A similar method of error minimization was applied for calibration of thermal power during cooling phase.

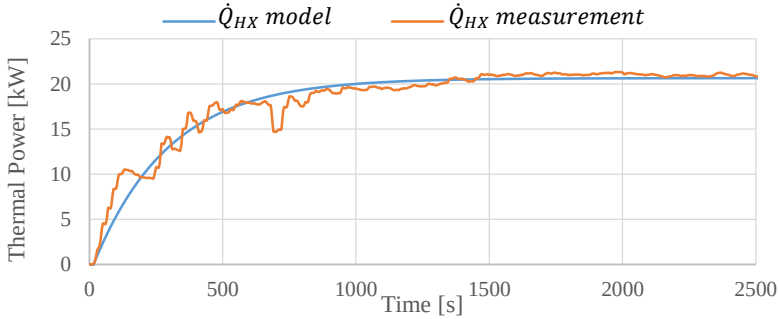

Fig. 7 Measured and modeled thermal power during a start-up phase

5. Discussion and conclusion

The three achievements of this paper can be summed up as:

- Performances measurements of an ICE µCHP with a condensing unit
- Validation of the genericity of the model for another technology
- Completion of a µCHP technology library based on a common model

The work done in this paper allowed to calibrate the dynamic model of a condensing ICE-µCHP unit. The performances in steady-state operation and dynamic conditions were explored and showed efficiencies significantly higher than standard non-condensing units available on the market for many years. Tests showed fast dynamic for electricity production which is promising to provide flexibility in smart-

grids. This work showed that the generic model developed a few years ago is convenient for one more technology providing that minor adjustments are made on the form of equations. Correctly led, eight days of tests should be enough to gather data to calibrate the model. It results in a completion of a library of multiple µCHP technologies (Stirling and steam Engines up to now, micro-turbine and fuel cells in the future) based on a common model that allow to compare performances thanks to simulation.

The next step of this work will be the simulation of various buildings, hydraulic configurations and controls to determine optimal integration of the ICE-unit in order to benefit from best achievable primary energy savings. The final objective is to provide recommendations on which type of technology the designer should choose and how to size and control the installation according to the building. The implementation in district simulation platform

Acknowledgment

The authors would like to thank Efficacity and Engie for financial support and COSTIC for providing the test facility.

References

[1] COGEN Europe, "COGEN Europe Position Paper, Micro-CHP – A cots effective solution save energy, reduce GHG emissions and partner with intermittent renewables," 2013.

[2] Dassault Systèmes, Dymola User Manual, 2014.

[3] V. Dorer and A. Weber, "Energy and CO 2 emissions performance assessment of residential micro-cogeneration systems with dynamic whole-building simulation programs," *Energy Conversion and Management*, no. 50, pp. 648-657, 2008.

[4] I. Beausoleil-Morrison, A. Ferguson, B. Griffith, N. Kelly, F. Maréchal and A. Weber, "Specifications for Modelling Fuel Cell and Combustion-Based Residential Cogeneration Devices within Whole-Building Simulation Programs," IEA, 2007.

[5] J.-B. Bouvenot, B. Andlauer, P. Stabat, D. Marchio and B. Flament, "Gas Stirling engine micro CHP boiler experimental data driven model for building energy simulation," *Energy and Buildings*, no. 84, pp. 117-131, 2014.

[6] J.-B. Bouvenot, B. Latour, M. Siroux, B. Flament, P. Stabat and D. Marchio, "Dynamic model based on experimental investigations of a wood pellet steam engine micro CHP for building energy simulation," *Applied Thermal Engineering*, vol. 73, pp. 1041-1054, 2014.

[7] I. Beausoleil-Morrison, "An Experimental and Simulation-Based Investigation of the Performance of Small-Scale Fuel Cell and Combustion-Based Cogeneration Devices Serving Residential Buildings," Government of Canada, Canada, 2008.

[8] B. Andlauer, Optimisation systémiques de micro-cogénérateurs intégrés au bâtiment, Paris: Ecole Nationale Supérieure des Mines de Paris, 2011.